Les Cahiers du GERAD ISSN: 0711–2440

Filtering for decentralized control in multi-agent interference coupled systems

M. Abedinpour Fallah, R. P. Malhamé,
D. Saussié, F. Martinelli

G–2017–04

January 2017

GERAD HEC Montréal
3000, chemin de la Côte-Sainte-Catherine
Montréal (Québec) Canada H3T 2A7

Tél. : 514 340-6053
Téléc. : 514 340-5665
info@gerad.ca
www.gerad.ca

Filtering for decentralized control in multi-agent interference coupled systems

Mehdi Abedinpour Fallah [a]
Roland P. Malhamé [a]
David Saussié [a]
Francesco Martinelli [b]

[a] *GERAD & the Department of Electrical Engineering, Polytechnique Montréal, Montreal (Québec), Canada*

[b] *Dipartimento di Ingegneria Civile e Ingegneria Informatica, Università di Roma "Tor Vergata", via del Politecnico, Rome, Italy*

mehdi.abedinpour-fallah@polymtl.ca
roland.malhame@polymtl.ca
david.saussie@polymtl.ca
francesco.martinelli@uniroma2.it

January 2017

Les Cahiers du GERAD
G–2017–04

Abstract: The object of study in the recent theory of Mean Field Games has been primarily large populations of agents interacting through a population dependent coupling term, entering through individual cost or dynamics. However, there are situations where agents are essentially independent, except for measurement interference. This is the case for example in cellular communications networked control across noisy channels. In previous work, we formulated the case of interference coupled linear partially observed stochastic agents as a game. Conditions were developed under which naively ignoring the interference term leads to asymptotically in population size, optimal control laws which are Riccati gain based. We tackle here the case of exact decentralized filtering under a class of time invariant certainty equivalent feedback controllers, and numerically investigate both stabilization ability and performance of such controllers as the state estimate feedback gain varies. While the optimum filters have memory requirements which become infinite over time, the stabilization ability of their finite memory approximation is also tested.

1 Introduction

Large population stochastic multi-agent systems have gained significant attention in the control community in recent years. This is due to the rich theory associated with decentralized control and system performance as well as to the growing number of important and challenging applications in control of networked dynamical systems, such as wireless sensor networks [1], very large scale robotics [2], controlled charging of a large population of electric vehicles [3], synchronization of coupled oscillators [4], swarm and flocking phenomenon in biological systems [5,6], evacuation of large crowds in emergency situations [7,8], sharing and competing for resources on the Internet [9], to cite a few. It is common in multi-agent systems to limit each individual agent in the system in terms of what it can decide on its own, what it can do on its own, and what it can measure on its own about its local environment. Owing to the limited sensing ability, it is not feasible for each individual agent to collect all other agents' state information, especially for large-scale dynamic systems. Therefore, the design of decentralized control and estimation laws depending only on local state measurements are required.

Several decentralized and distributed estimation schemes for large-scale systems have been proposed to make the estimation problem computationally efficient. In [10,11] distributed and decentralized approaches to state estimation and control were developed for large-scale multi-rate systems with applications to power networks and plantwide processes, respectively. In [12–16] distributed decision-making with partial observation for large population stochastic multi-agent systems was studied, where the synthesis of Nash strategies was investigated for the agents that are weakly coupled through either individual dynamics or costs.

In previous work [17], the case of N uniform agents described by linear stochastic dynamics with quadratic costs and partial linear observations involving the mean of all agents was considered, and the problem was formulated as an interference induced game. We explored conditions under which a Luenberger like observer, together with a constant state feedback in individual systems would be: (i) ideally optimal, (ii) at least stable. Our objective in the current paper is to extend the class of candidate stabilizing control structures via optimal filtering. In particular, we study the optimal decentralized filtering problem under a class of certainty equivalent controllers, and numerically investigate both stabilization ability and performance of such controllers as the state estimate feedback gain varies. While the optimum filters have memory requirements which become infinite over time, the stabilization ability of their finite memory approximation is also tested.

The rest of the paper is organized as follows. The problem is defined and formulated in Section 2. A summary of the previous work [17] is given at the start of Section 3, followed by detailed derivations of the optimal growing dimension filter and associated approximate finite memory filters. In Section 4, both stabilization ability and performance of this class of state estimate feedback controllers are numerically investigated. Section 5 presents an application example for a class of networked multi-agent control systems. Concluding remarks are stated in Section 6.

2 Model formulation and problem statement

Consider a system of N agents, with individual scalar dynamics for simplicity of computations. The evolution of the state component is described by

$$x_{k+1,i} = ax_{k,i} + bu_{k,i} + w_{k,i}, \tag{1}$$

with partial scalar state observations given by

$$y_{k,i} = cx_{k,i} + h\left(\frac{1}{N}\sum_{j=1}^{N} x_{k,j}\right) + v_{k,i}, \tag{2}$$

for $k \geq 0$ and $1 \leq i \leq N$, where $x_{k,i}, u_{k,i}, y_{k,i} \in \mathbb{R}$ are the state, the control input and the measured output of the i^{th} agent, respectively. The random variables $w_{k,i} \sim \mathcal{N}(0, \sigma_w^2)$ and $v_{k,i} \sim \mathcal{N}(0, \sigma_v^2)$ represent independent Gaussian white noises at different times k and at different agents i. The Gaussian initial conditions $x_{0,i} \sim \mathcal{N}(\bar{x}_0, \sigma_0^2)$ are mutually independent and are also independent of $\{w_{k,i}, v_{k,i}, 1 \leq i \leq N,\, k \geq 0\}$. σ_w^2, σ_v^2 and σ_0^2

denote the variance of $w_{k,i}$, $v_{k,i}$ and $x_{0,i}$, respectively. Moreover, a is a scalar parameter and $b, c, h > 0$ are positive scalar parameters. In addition, the individual cost function for each agent is given by

$$J_i \triangleq \overline{\lim_{T\to\infty}} \frac{1}{T}\mathbb{E}\sum_{k=0}^{T-1}(x_{k,i}^2 + r u_{k,i}^2). \tag{3}$$

where $r > 0$ is a positive scalar parameter, $\mathbb{E}\{.\}$ is the expectation operator, and $\overline{\lim}$ is $\limsup$.

The problem to be considered is to develop decentralized estimation policies such that each agent is stabilized by a linear feedback control of the form

$$u_{k,i} = -f\hat{x}_{k,i}, \tag{4}$$

where f is a constant scalar gain, and $\hat{x}_{k,i}$ is an estimator of $x_{k,i}$ based only on observations of the i^{th} agent. More specifically, the control is a linear feedback $-f\hat{x}_{k,i}$ on the state estimate of $x_{k,i}$, while the state estimate $\hat{x}_{k,i}$ is obtained based solely on agent i's own observations $y_{k,i}$, $y_{k-1,i}$, $y_{k-2,i}$, $y_{k-3,i}$, ...

3 Filtering for a class of certainty equivalent controllers

3.1 Previous work

In [17], we explored the conditions under which a Luenberger like observer of the form

$$\hat{x}_{k+1,i} = (a-bf)\hat{x}_{k,i} + K(y_{k+1,i} - c(a-bf)\hat{x}_{k,i}), \tag{5}$$

together with a constant state estimate feedback in individual systems would be: (i) ideally optimal, (ii) at least stable. It was found that (i) was asymptotically true (as N goes to infinity) when state gain a is less than a value called a_{Nash} and which can be exactly computed. Up to a_{Nash}, the optimum control policy is the isolated (naive) Kalman gain K^* (obtained by assuming zero interference in the local measurements, i.e., setting $h = 0$ in (2)) combined with the Riccati dictated optimal gain f^*, with

$$K^*(a) = \frac{cP_\infty(a)}{c^2P_\infty(a) + \sigma_v^2}, \tag{6}$$

where $P_\infty(a)$ is the unique positive solution of

$$c^2P_\infty^2(a) + ((1-a^2)\sigma_v^2 - c^2\sigma_w^2)P_\infty(a) - \sigma_w^2\sigma_v^2 = 0, \tag{7}$$

and

$$f^*(a,r) = \frac{ab\Sigma_\infty}{b^2\Sigma_\infty + r}, \tag{8}$$

where Σ_∞ is the positive solution of the algebraic Riccati equation

$$b^2\Sigma_\infty^2 + (r - a^2r - b^2)\Sigma_\infty - r = 0. \tag{9}$$

There is also a_{sup} greater than a_{Nash} such that when a is between a_{Nash} and a_{sup}, one can reverse engineer a range of coefficients r for the cost functions in (3) for which the naive Kalman gain K^* combined with the feedback gain f^* dictated by the Riccati equation will be asymptotically optimal. Finally, past a_{sup}, no optimal control interpretation is possible any more, although there exist couples (K, f) which may still stabilize the system up to a maximum value, and only cooperatively chosen common gains can get us to approach a minimum cost. Let a_s be the limit past which constant Luenberger like observer and feedback gains can no longer stabilize the system. The current paper is a continuation of stabilization and optimality investigations for values of a past a_s.

From [17], for each fixed a it is possible to stabilize the system using a Luenberger like observer Equation (5) and the pair (K, f) if and only if (K, f) is in a stability region denoted by $S(a)$, independent of N. Let $a_f = a - bf$, and also let $a_m(f)$ (or equivalently $a_m(a_f)$) denote the maximum value of a such that $(K^*(a), a_f) \in S(a)$ for some $a_f \in [0, 1)$. Moreover, let $a_m = \sup_{a_f\in[0,1)} a_m(a_f)$. Then we have the following numerical results.

3.1.1 Numerical results

The numerical results reported in this paper are obtained considering the following parameter setting: $b = c = h = 1$ and $\sigma_w = \sigma_v = \sigma_0 = 1$, with $\mathbb{E}x_{0,i} = \bar{x}_0 = 0$ for all agents $i = 1, 2, \ldots, N$. In addition, we will only deal with the case $a \geq 0$ (a symmetric property holds for the $a \leq 0$ case). The value of a and f will be specified in the different simulations.

By numerical investigation we have $a_m \approx 3.6$ which is obtained by letting a_f go to 1. Figure 1 is a representation of the stability regions for the assumed parameter setting when a varies from $a = 0.2$ to $a_s = 5.5$. It is observed that the stability region gradually shrinks as a increases until it all but vanishes at $a_s = 5.5$. More specifically, for all $a < a_{Nash}$, all intersections of the horizontal line $K^*(a)$ with all the vertical lines (marking values of f which, given a , satisfy (8) for some value of input penalty coefficient r, where r goes from 0 to infinity) belong to the stability region. For all $a \in (a_{Nash}, a_{sup})$ this holds only for large enough r while for $a = a_{sup}$ all the intersections cease to belong to the brown area. For $a = a_m$ the Kalman gain ceases to be in the stability region for all $a_f \in [0, 1)$ and, for $a = 5.5$ the stability region becomes empty.

3.2 Exact optimal bulk filter

The goal of this section is to extend the class of candidate stabilizing control structures via *exact* optimal filtering with $h \neq 0$ in its formulation. In particular, when local state estimate feedback (4) is included in the i^{th} agent state Equation (1), the result is as follows:

$$x_{k+1,i} = ax_{k,i} - bf\hat{x}_{k,i} + w_{k,i}. \tag{10}$$

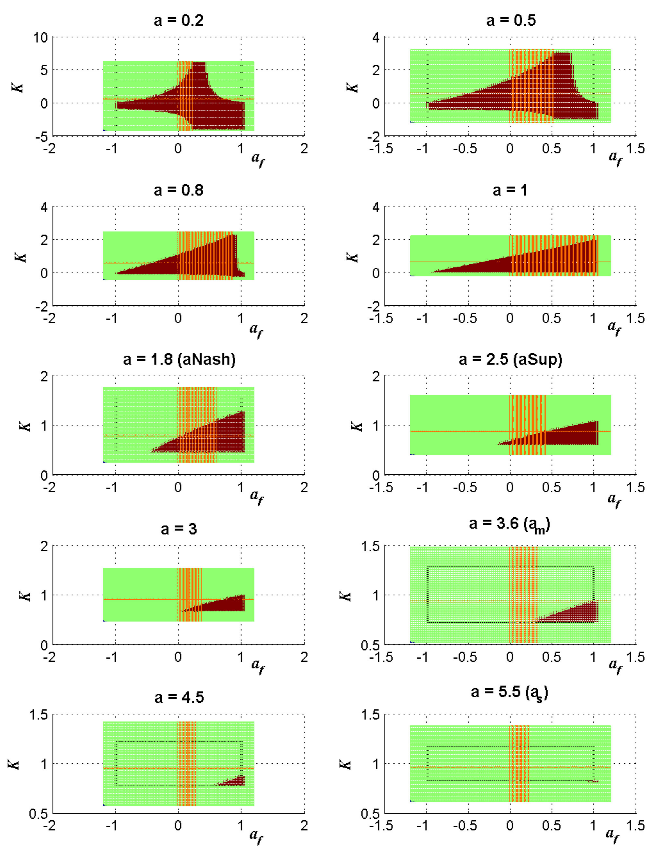

Figure 1: The stability regions $S(a)$ (brown shaded areas) in the (K, a_f) plane. The vertical lines represent the optimal Riccati gain $f^*(a, r)$ corresponding to all possible values of parameter r while the horizontal line is the optimal isolated (naive) Kalman filter gain $K^*(a)$.

In addition, anticipating the need to account for the influence of average states in the dynamics through the measurement equation, and letting a tilde $(\tilde{.})$ indicate an averaging over agents operation, we define:

$$m_k = \frac{1}{N}\sum_{j=1}^{N} x_{k,j}, \quad \tilde{m}_k = \frac{1}{N}\sum_{j=1}^{N} \hat{x}_{k,j}, \tag{11}$$

$$\tilde{w}_k = \frac{1}{N}\sum_{j=1}^{N} w_{k,j}, \quad \tilde{v}_k = \frac{1}{N}\sum_{j=1}^{N} v_{k,j}. \tag{12}$$

Thus, combining (10), (11), (12), we obtain:

$$m_{k+1} = am_k - bf\tilde{m}_k + \tilde{w}_k \tag{13}$$

It appears that optimal decentralized estimation in our problem structure, does not lend itself naturally to a recursive computation. Indeed, the sufficient statistic from the past (adequate state description) appears to grow by 2 components at every step. More specifically, average agent state (averaging over all agents) and average agent state estimate enter into the dynamics of the controlled individual agents, through the $-f\hat{x}_{k,i}$ term into the dynamics (1), and thus the dynamics of both of these averages must be specified to complete the estimation procedure. As a result, one has to augment the dynamics of (1) by at least that of the agents states average term in the estimation at the first step. When optimal filtering is applied to the augmented state, computations of both the innovation term and its gain involve an expected value of the average state and the average state estimate (because the latter enters the average agent state dynamics). This yields to the apparent infinite regress effect.

A significant source of complexity in the analysis, is self dependency of filtering equations. Roughly speaking, since the averaged agent state enters into individual measurements, the effective stochasticity in a single agent's measurements depends on how precisely other agents are estimating their individual states. Thus by symmetry, the level of uncertainty in individual state estimates depends on itself. Furthermore, the straightforward recursive Kalman filter assumes that the internal and measurement sequences noises are uncorrelated with their past (white noise property). However, in the sequence of expanding state models that we need to construct for estimation purposes as the time index increases, the noise vectors are also expanding, and are partially common from one stage to another.

However, given that all noise and initial random variables are jointly Gaussian and noting that linearity is preserved in our control structure set up, optimal estimates will be linear functions of the measurements. Hence, using the classical Gaussian unbiased minimum variance estimation theory [18], we derive the exact optimal growing dimension filter whereby at every time step, all past and present available measurements are considered. In particular, let us denote by K_k the time-varying $1 \times k$ row vector of filter gains necessary for computing $\hat{x}_{k,i}$. Also let $Y_{1,i}^k$ indicate the column vector of all measurements up to time k at agent i. The minimum covariance estimator $\hat{x}_{k,i}$ minimizes the mean square estimation error

$$\Sigma_k = \mathbb{E}\left[\left(x_{k,i} - \hat{x}_{k,i}\right)^2 | Y_{1,i}^k\right], \tag{14}$$

and is given by the exact growing dimension filter (the optimal Bulk filter) equations [18, 19]:

$$\hat{x}_{k,i} = \mathbb{E}\left[x_{k,i}\right] + K_k\left(Y_{1,i}^k - \mathbb{E}\left[Y_{1,i}^k\right]\right), \tag{15}$$

$$\Sigma_k = P_{x_{k,i}x_{k,i}} - K_k P_{x_{k,i}Y_{1,i}^k}^T, \tag{16}$$

with optimal time-varying gain

$$K_k = P_{x_{k,i}Y_{1,i}^k} P_{Y_{1,i}^k Y_{1,i}^k}^{-1}, \tag{17}$$

where

$$P_{x_{k,i}Y_{1,i}^k} = \mathbb{E}\left[\left(x_{k,i} - \mathbb{E}\left[x_{k,i}\right]\right)\left(Y_{1,i}^k - \mathbb{E}\left[Y_{1,i}^k\right]\right)^T\right], \tag{18}$$

$$P_{Y_{1,i}^k Y_{1,i}^k} = \mathbb{E}\left[\left(Y_{1,i}^k - \mathbb{E}\left[Y_{1,i}^k\right]\right)\left(Y_{1,i}^k - \mathbb{E}\left[Y_{1,i}^k\right]\right)^T\right]. \tag{19}$$

The next theorem gives a semi-recursive computational scheme for the exact growing dimension filter (15)–(17), which uses all of the results from previous cycles up to time $k-1$ to compute K_k in one shot.

Theorem 1 *The optimal decentralized state estimator* $\hat{x}_{k,i}$ *is given by:*

$$\hat{x}_{k,i} = (a-bf)^k \bar{x}_0 + K_k \begin{bmatrix} y_{1,i} - (c+h)(a-bf)\bar{x}_0 \\ y_{2,i} - (c+h)(a-bf)^2\bar{x}_0 \\ \vdots \\ y_{k,i} - (c+h)(a-bf)^k\bar{x}_0 \end{bmatrix}, \tag{20}$$

with optimal time-varying gain K_k*, obtained from Levinson-like order-updating relations given by:*

$$K_k = \left[(a-bf)K_{k-1} \quad 0\right] + \frac{P_{x_{k,i}y_{k,i}} - P_{x_{k,i}Y_{1,i}^{k-1}} P^{-1}_{Y_{1,i}^{k-1}Y_{1,i}^{k-1}} P_{Y_{1,i}^{k-1}y_{k,i}}}{P_{y_{k,i}y_{k,i}} - P^T_{Y_{1,i}^{k-1}y_{k,i}} P^{-1}_{Y_{1,i}^{k-1}Y_{1,i}^{k-1}} P_{Y_{1,i}^{k-1}y_{k,i}}} \left[-P^T_{Y_{1,i}^{k-1}y_{k,i}} P^{-1}_{Y_{1,i}^{k-1}Y_{1,i}^{k-1}} \quad 1\right], \tag{21}$$

with $K_1 = P_{x_{1,i}y_{1,i}}/P_{y_{1,i}y_{1,i}}$*, and*

$$P^{-1}_{Y_{1,i}^{k}Y_{1,i}^{k}} = \begin{bmatrix} P^{-1}_{Y_{1,i}^{k-1}Y_{1,i}^{k-1}} & 0_{(k-1)\times 1} \\ 0_{1\times(k-1)} & 0 \end{bmatrix} + \frac{1}{P_{y_{k,i}y_{k,i}} - P^T_{Y_{1,i}^{k-1}y_{k,i}} P^{-1}_{Y_{1,i}^{k-1}Y_{1,i}^{k-1}} P_{Y_{1,i}^{k-1}y_{k,i}}} \begin{bmatrix} -P^{-1}_{Y_{1,i}^{k-1}Y_{1,i}^{k-1}} P_{Y_{1,i}^{k-1}y_{k,i}} \\ 1 \end{bmatrix} \begin{bmatrix} -P^{-1}_{Y_{1,i}^{k-1}Y_{1,i}^{k-1}} P_{Y_{1,i}^{k-1}y_{k,i}} \\ 1 \end{bmatrix}^T, \tag{22}$$

where the covariances $P_{x_{k,i}y_{t,i}}$ *and* $P_{y_{k,i}y_{t,i}}$ *are respectively defined as*

$$P_{x_{k,i}y_{t,i}} = \mathbb{E}\left[\left(x_{k,i} - \mathbb{E}\left[x_{k,i}\right]\right)\left(y_{t,i} - \mathbb{E}\left[y_{t,i}\right]\right)^T\right], \tag{23}$$

$$P_{y_{k,i}y_{t,i}} = \mathbb{E}\left[\left(y_{k,i} - \mathbb{E}\left[y_{k,i}\right]\right)\left(y_{t,i} - \mathbb{E}\left[y_{t,i}\right]\right)^T\right], \tag{24}$$

for $t = 1, ..., k$*, and are obtained recursively from the following equations:*

$$P_{x_{k,i}y_{t,i}} = \begin{cases} aP_{x_{k-1,i}y_{t,i}} - bfK_{k-1} \begin{bmatrix} P_{y_{1,i}y_{t,i}} \\ \vdots \\ P_{y_{k-1,i}y_{t,i}} \end{bmatrix}, & \text{for } t = 1, \ldots, k-1 \\ cP_{x_{k,i}x_{t,i}} + hP_{x_{k,i}m_t}, & \text{for } t \geq k \end{cases} \tag{25}$$

$$P_{y_{k,i}y_{t,i}} = \begin{cases} cP_{x_{k,i}y_{t,i}} + hP_{y_{t,i}m_k}, & \text{for } t = 1, \ldots, k-1 \\ cP_{x_{k,i}y_{k,i}} + hP_{y_{k,i}m_k} + \sigma_v^2, & \text{for } t = k \end{cases} \tag{26}$$

$$P_{y_{k,i}m_t} = \begin{cases} cP_{x_{k,i}m_t} + hP_{m_k m_t}, & \text{for } t \leq k \\ aP_{y_{k,i}m_{t-1}} - bfK_{t-1} \begin{bmatrix} (c+h)P_{y_{k,i}m_1} + P_{y_{k,i}\tilde{v}_1} \\ \vdots \\ (c+h)P_{y_{k,i}m_{t-1}} + P_{y_{k,i}\tilde{v}_{t-1}} \end{bmatrix}, & \text{for } t > k \end{cases} \tag{27}$$

$$P_{x_{k,i}x_{t,i}} = \begin{cases} aP_{x_{k-1,i}x_{t,i}} \\ -bfK_{k-1} \begin{bmatrix} P_{x_{t,i}y_{1,i}} \\ \vdots \\ P_{x_{t,i}y_{k-1,i}} \end{bmatrix}, & \text{for } t = 1, \ldots, k-1 \\ a^2 P_{x_{k-1,i}x_{k-1,i}} - 2abfK_{k-1} \begin{bmatrix} P_{x_{k-1,i}y_{1,i}} \\ \vdots \\ P_{x_{k-1,i}y_{k-1,i}} \end{bmatrix} + b^2 f^2 K_{k-1} P_{Y_{1,i}^{k-1}Y_{1,i}^{k-1}} K_{k-1}^T + \sigma_w^2, & \text{for } t = k \end{cases} \tag{28}$$

$$P_{x_{k,i}m_t} = \begin{cases} aP_{x_{k-1,i}m_t} - bfK_{k-1}\begin{bmatrix} P_{y_{1,i}m_t} \\ \vdots \\ P_{y_{k-1,i}m_t} \end{bmatrix}, & \textit{for } t = 1,\dots,k-1 \\ a^2P_{x_{k-1,i}m_{t-1}} - abf(c+h)K_{k-1}\begin{bmatrix} P_{x_{k-1,i}m_1} \\ \vdots \\ P_{x_{k-1,i}m_{t-1}} \end{bmatrix} & \\ -abfK_{k-1}\begin{bmatrix} P_{x_{k-1,i}\tilde{v}_1} \\ \vdots \\ P_{x_{k-1,i}\tilde{v}_{t-1}} \end{bmatrix} - abfK_{k-1}\begin{bmatrix} P_{y_{1,i}m_{t-1}} \\ \vdots \\ P_{y_{k-1,i}m_{t-1}} \end{bmatrix} & \\ +b^2f^2K_{k-1}((c+h)P_{Y_{1,i}^{k-1}M_1^{t-1}} + P_{Y_{1,i}^{k-1}\tilde{V}_1^{t-1}})K_{k-1}^T & \\ +aP_{x_{k-1,i}\tilde{w}_{t-1}} + aP_{m_{t-1}w_{k-1,i}} - bfK_{k-1}\begin{bmatrix} P_{y_{1,i}\tilde{w}_{t-1}} \\ \vdots \\ P_{y_{k-1,i}\tilde{w}_{t-1}} \end{bmatrix} & \\ -bf(c+h)K_{k-1}\begin{bmatrix} P_{m_1w_{k-1,i}} \\ \vdots \\ P_{m_{t-1}w_{k-1,i}} \end{bmatrix} + P_{w_{k-1,i}\tilde{w}_{t-1}} & \textit{for } t \geq k \end{cases} \tag{29}$$

$$P_{m_km_t} = \begin{cases} aP_{m_{k-1}m_t} - bfK_{k-1}\begin{bmatrix} (c+h)P_{m_1m_t} + P_{m_t\tilde{v}_1} \\ \vdots \\ (c+h)P_{m_{k-1}m_t} + P_{m_t\tilde{v}_{k-1}} \end{bmatrix}, & \textit{for } t = 1,\dots,k-1 \\ a^2P_{m_{k-1}m_{k-1}} - 2abf(c+h)K_{k-1}\begin{bmatrix} P_{m_{k-1}m_1} \\ \vdots \\ P_{m_{k-1}m_{k-1}} \end{bmatrix} & \\ -2abfK_{k-1}\begin{bmatrix} P_{m_{k-1}\tilde{v}_1} \\ \vdots \\ P_{m_{k-1}\tilde{v}_{k-1}} \end{bmatrix} + b^2f^2K_{k-1}((c+h)^2 & \\ P_{M_1^{k-1}M_1^{k-1}} + (c+h)(P_{M_1^{k-1}\tilde{V}_1^{k-1}} + P^T_{M_1^{k-1}\tilde{V}_1^{k-1}}) + P_{\tilde{V}_1^{k-1}\tilde{V}_1^{k-1}})K_{k-1}^T + \frac{\sigma_w^2}{N}, & \textit{for } t = k \end{cases} \tag{30}$$

$$P_{y_{k,i}w_{t,i}} = cP_{x_{k,i}w_{t,i}} + hP_{m_kw_{t,i}}, \tag{31}$$

$$P_{m_kw_{t,i}} = \begin{cases} 0, & \textit{for } t > k-1 \\ \frac{\sigma_w^2}{N}, & \textit{for } t = k-1 \\ aP_{m_{k-1}w_{t,i}} - bf(c+h)K_{k-1}\begin{bmatrix} P_{m_1w_{t,i}} \\ \vdots \\ P_{m_{k-1}w_{t,i}} \end{bmatrix}, & \textit{for } t < k-1 \end{cases} \tag{32}$$

$$P_{x_{k,i}w_{t,i}} \begin{cases} 0, & \textit{for } t > k-1 \\ \sigma_w^2, & \textit{for } t = k-1 \\ aP_{x_{k-1,i}w_{t,i}} - bfK_{k-1}\begin{bmatrix} cP_{x_{1,i}w_{t,i}} + hP_{m_1w_{t,i}} \\ \vdots \\ cP_{x_{k-1,i}w_{t,i}} + hP_{m_{k-1}w_{t,i}} \end{bmatrix}, & \textit{for } t < k-1 \end{cases} \tag{33}$$

$$P_{y_{k,i}\tilde{w}_t} = cP_{x_{k,i}\tilde{w}_t} + hP_{m_k\tilde{w}_t}, \tag{34}$$

$$P_{m_k\tilde{w}_t} = \begin{cases} 0, & for\ t > k-1 \\ \frac{\sigma_w^2}{N}, & for\ t = k-1 \\ aP_{m_{k-1}\tilde{w}_t} - bf(c+h)K_{k-1}\begin{bmatrix} P_{m_1\tilde{w}_t} \\ \vdots \\ P_{m_{k-1}\tilde{w}_t} \end{bmatrix}, & for\ t < k-1 \end{cases} \tag{35}$$

$$P_{x_{k,i}\tilde{w}_t} = \begin{cases} 0, & for\ t > k-1 \\ \frac{\sigma_w^2}{N}, & for\ t = k-1 \\ aP_{x_{k-1,i}\tilde{w}_t} - bfK_{k-1}\begin{bmatrix} cP_{x_{1,i}\tilde{w}_t} + hP_{m_1\tilde{w}_t} \\ \vdots \\ cP_{x_{k-1,i}\tilde{w}_t} + hP_{m_{k-1}\tilde{w}_t} \end{bmatrix}, & for\ t < k-1 \end{cases} \tag{36}$$

$$P_{y_{k,i}v_{t,i}} = \begin{cases} 0, & for\ t > k \\ \sigma_v^2, & for\ t = k \\ cP_{x_{k,i}v_{t,i}} + hP_{m_k v_{t,i}}, & for\ t < k \end{cases} \tag{37}$$

$$P_{m_k v_{t,i}} = \begin{cases} 0, & for\ t > k-1 \\ -bfK_{k-1}(k-1)\frac{\sigma_v^2}{N}, & for\ t = k-1 \\ aP_{m_{k-1}v_{t,i}} - bfK_{k-1}(t)\frac{\sigma_v^2}{N} - bf(c+h)K_{k-1}\begin{bmatrix} P_{m_1 v_{t,i}} \\ \vdots \\ P_{m_{k-1}v_{t,i}} \end{bmatrix}, & for\ t < k-1 \end{cases} \tag{38}$$

$$P_{x_{k,i}v_{t,i}} = \begin{cases} 0, & for\ t > k-1 \\ -bfK_{k-1}(k-1)\sigma_v^2, & for\ t = k-1 \\ aP_{x_{k-1,i}v_{t,i}} - bfK_{k-1}(t)\sigma_v^2 - bfK_{k-1}\begin{bmatrix} cP_{x_{1,i}v_{t,i}} + hP_{m_1 v_{t,i}} \\ \vdots \\ cP_{x_{k-1,i}v_{t,i}} + hP_{m_{k-1}v_{t,i}} \end{bmatrix}, & for\ t < k-1 \end{cases} \tag{39}$$

$$P_{y_{k,i}\tilde{v}_t} = \begin{cases} 0, & for\ t > k \\ \frac{\sigma_v^2}{N}, & for\ t = k \\ cP_{x_{k,i}\tilde{v}_t} + hP_{m_k\tilde{v}_t}, & for\ t < k \end{cases} \tag{40}$$

$$P_{m_k\tilde{v}_t} = \begin{cases} 0, & for\ t > k-1 \\ -bfK_{k-1}(k-1)\frac{\sigma_v^2}{N}, & for\ t = k-1 \\ aP_{m_{k-1}\tilde{v}_t} - bfK_{k-1}(t)\frac{\sigma_v^2}{N} - bf(c+h)K_{k-1}\begin{bmatrix} P_{m_1\tilde{v}_t} \\ \vdots \\ P_{m_{k-1}\tilde{v}_t} \end{bmatrix}, & for\ t < k-1 \end{cases} \tag{41}$$

$$P_{x_{k,i}\tilde{v}_t} = \begin{cases} 0, & for\ t > k-1 \\ -bfK_{k-1}(k-1)\frac{\sigma_v^2}{N}, & for\ t = k-1 \\ aP_{x_{k-1,i}\tilde{v}_t} - bfK_{k-1}(t)\frac{\sigma_v^2}{N} - bfK_{k-1}\begin{bmatrix} cP_{x_{1,i}\tilde{v}_t} + hP_{m_1\tilde{v}_t} \\ \vdots \\ cP_{x_{k-1,i}\tilde{v}_t} + hP_{m_{k-1}\tilde{v}_t} \end{bmatrix}, & for\ t < k-1 \end{cases} \tag{42}$$

where $K_k(j)$ denotes the j^{th} element of K_k, and M_1^k, $\tilde{V}_1^k$ respectively indicate the column vector of m and $\tilde{v}$ from time 1 up to time k.

Proof. See the Appendix. □

Remark 1 *Note that the Bulk filter estimation at step k requires solving* all the intermediate steps *from* 1 *to k, because this is a situation of* dual control *whereby the quality of estimation at time step k depends on previous control actions, themselves a function of previous filtering results.*

Remark 2 *Note also that all the above expressions capitalize on computations already carried out at the previous time step; otherwise, the complexity of calculations would make bulk filtering estimates an essentially insurmountable task.*

The next Lemma gives the cross covariance of two arbitrary agents.

Lemma 1 *The cross covariance of two arbitrary agents $x_{k,i}$ and $x_{k,j}$ over time are obtained recursively from the following equations:*

$$P_{x_{k,i}x_{t,j}} = \begin{cases} aP_{x_{k-1,i}x_{t,j}} - bfK_{k-1}\begin{bmatrix} P_{x_{t,j}y_{1,i}} \\ \vdots \\ P_{x_{t,j}y_{k-1,i}} \end{bmatrix}, & \textit{for } t = 1,\dots,k-1 \\ a^2 P_{x_{k-1,i}x_{k-1,j}} - abfK_{k-1}\begin{bmatrix} P_{x_{k-1,i}y_{1,j}} \\ \vdots \\ P_{x_{k-1,i}y_{k-1,j}} \end{bmatrix} - abfK_{k-1} & \\ \begin{bmatrix} P_{x_{k-1,j}y_{1,i}} \\ \vdots \\ P_{x_{k-1,j}y_{k-1,i}} \end{bmatrix} + b^2f^2K_{k-1}P_{Y_{1,i}^{k-1}Y_{1,j}^{k-1}}K_{k-1}^T, & \textit{for } t = k \end{cases} \tag{43}$$

where

$$P_{x_{k,i}y_{t,j}} = \begin{cases} aP_{x_{k-1,i}y_{t,j}} - bfK_{k-1}\begin{bmatrix} P_{y_{1,i}y_{t,j}} \\ \vdots \\ P_{y_{k-1,i}y_{t,j}} \end{bmatrix}, & \textit{for } t < k \\ cP_{x_{k,i}x_{t,j}} + hP_{x_{k,i}m_t}, & \textit{for } t \geq k \end{cases} \tag{44}$$

$$P_{y_{k,i}y_{t,j}} = cP_{x_{k,i}y_{t,j}} + hP_{y_{t,j}m_k}, \qquad \textit{for } t = 1,\dots,k \tag{45}$$

Proof. See the Appendix. □

3.3 Finite memory filtering approximations

The optimal Bulk filter is an infinite impulse response (IIR) filter. Any stable IIR filter can be approximated to any desirable degree by a finite impulse response (FIR) filter [20]. In this section, we derive approximate finite-dimensional (time-varying) filters to reduce memory requirements of the Bulk filter. Let any variable with superscript (n) correspond to an approximate FIR filter of length n, where only the last n measurements are preserved. In particular, let us denote by $K_k^{(n)}$ the time-varying $1 \times n$ row vector of filter gains necessary for computing $\hat{x}_{k,i}^{(n)}$. Also let $Y_{k-n+1,i}^k$ indicate the column vector of n measurements from time $k-n+1$ up to time k at agent i, and assume zero mean for initial conditions of all agents, i.e., $\mathbb{E}x_{0,i} = \bar{x}_0 = 0, i \geq 1$. The minimum covariance estimator $\hat{x}_{k,i}^{(n)}$ minimizes the mean square estimation error

$$\Sigma_k^{(n)} = \mathbb{E}\left[\left(x_{k,i} - \hat{x}_{k,i}^{(n)}\right)^2 |Y_{k-n+1,i}^k\right], \tag{46}$$

and is given by [20]:

$$\hat{x}_{k,i}^{(n)} = K_k^{(n)} Y_{k-n+1,i}^k, \tag{47}$$

$$\Sigma_k^{(n)} = P_{x_{k,i}x_{k,i}} - K_k^{(n)} P^T_{x_{k,i}Y^k_{k-n+1,i}}, \tag{48}$$

with optimum time-varying gain

$$K_k^{(n)} = P_{x_{k,i}Y^k_{k-n+1,i}} P^{-1}_{Y^k_{k-n+1,i}Y^k_{k-n+1,i}}. \tag{49}$$

The next theorem gives a semi-recursive computational scheme for the optimum finite memory filter (47)–(49), which uses all of the results from time $k-n$ up to time $k-1$ to compute $K_k^{(n)}$ in one shot.

Theorem 2 *The approximate optimal decentralized state estimator $\hat{x}_{k,i}^{(n)}$ is given by:*

$$\hat{x}_{k,i}^{(n)} = K_k^{(n)} Y_{k-n+1,i}^k, \tag{50}$$

with optimal time-varying gain $K_k^{(n)}$, obtained from Levinson-like order-updating relations given by:

$$K_k^{(l+1)} = \begin{bmatrix} 0 & K_k^{(l)} \end{bmatrix} + \frac{P_{x_{k,i}y_{k-l,i}} - P_{x_{k,i}Y^k_{k-l+1,i}} P^{-1}_{Y^k_{k-l+1,i}Y^k_{k-l+1,i}} P^T_{y_{k-l,i}Y^k_{k-l+1,i}}}{P_{y_{k-l,i}y_{k-l,i}} - P_{y_{k-l,i}Y^k_{k-l+1,i}} P^{-1}_{Y^k_{k-l+1,i}Y^k_{k-l+1,i}} P^T_{y_{k-l,i}Y^k_{k-l+1,i}}} \begin{bmatrix} 1 & -P_{y_{k-l,i}Y^k_{k-l+1,i}} P^{-1}_{Y^k_{k-l+1,i}Y^k_{k-l+1,i}} \end{bmatrix}, \tag{51}$$

for $l = 1, ..., n-1$, with $K_k^{(1)} = P_{x_{k,i}y_{k,i}}/P_{y_{k,i}y_{k,i}}$, and

$$P^{-1}_{Y^k_{k-l,i}Y^k_{k-l,i}} = \begin{bmatrix} 0 & 0_{1\times l} \\ 0_{l\times 1} & P^{-1}_{Y^k_{k-l+1,i}Y^k_{k-l+1,i}} \end{bmatrix} + \frac{1}{P_{y_{k-l,i}y_{k-l,i}} - P_{y_{k-l,i}Y^k_{k-l+1,i}} P^{-1}_{Y^k_{k-l+1,i}Y^k_{k-l+1,i}} P^T_{y_{k-l,i}Y^k_{k-l+1,i}}} \begin{bmatrix} 1 \\ -P^{-1}_{Y^k_{k-l+1,i}Y^k_{k-l+1,i}} P^T_{y_{k-l,i}Y^k_{k-l+1,i}} \end{bmatrix} \begin{bmatrix} 1 \\ -P^{-1}_{Y^k_{k-l+1,i}Y^k_{k-l+1,i}} P^T_{y_{k-l,i}Y^k_{k-l+1,i}} \end{bmatrix}^T, \tag{52}$$

for $l = 1, ..., n-1$, where the covariances $P_{x_{k,i}y_{t,i}}$ and $P_{y_{k,i}y_{t,i}}$ are obtained recursively from the truncated covariance expressions (25)–(42) by considering $k-n+1 \le t \le k$, and replacing K_k with $K_k^{(n)}$.

Proof. See the Appendix. □

3.4 The steady state isolated Kalman sequence

In this section, we obtain the equivalent sequence for the isolated Kalman filter equation in the steady-state.

Proposition 1 *In the stability region, the isolated Kalman filter equivalent equation in the steady-state is given by*

$$\hat{x}_{k,i} = K'_1 y_{k,i} + K'_2 y_{k-1,i} + ... + K'_k y_{1,i}, \tag{53}$$

where

$$
\begin{aligned}
K_1' =& K^*, && (54)\\
K_2' =& (a-bf)(1-cK^*)K^*, && (55)\\
K_3' =& (a-bf)^2(1-cK^*)^2K^*, && (56)\\
K_4' =& (a-bf)^3(1-cK^*)^3K^*, \textit{ and so on....} && (57)
\end{aligned}
$$

Proof. Let K be given as (6) in (5). By rearranging (5) we have:

$$\hat{x}_{k+1,i} = (a-bf)(1-cK^*)\hat{x}_{k,i} + K^*y_{k+1,i}. \tag{58}$$

Then substituting

$$\hat{x}_{k,i} = K_1'y_{k,i} + K_2'y_{k-1,i} + ... + K_k'y_{1,i}, \tag{59}$$

and

$$\hat{x}_{k+1,i} = K_1'y_{k+1,i} + K_2'y_{k,i} + ... + K_{k+1}'y_{1,i}, \tag{60}$$

into (58) and applying the stationarity property by making the left-hand-side of the resulting equation equal to its right-hand-side, we get the fixed-point values (54)–(57). □

4 Numerical study of filtering and control performance

In this section, we numerically investigate state tracking ability of both the exact (growing dimension) bulk filter and its approximate finite dimension versions, as well as the control performance of the associated certainty equivalent controllers.

4.1 Stabilization ability of certainty equivalent controllers

First, we numerically demonstrate the stabilization ability of our class of certainty equivalent controllers using an arbitrary feedback gain f such that $|a_f| < 1$ (where $a_f = a - bf$) on the bulk filter estimate. In particular, Figures 2, 3 and 4 respectively, show the stable behavior of a representative agent (namely, the 50^{th} agent) when $a = 10$, $a = 100$, and $a = 1000$.

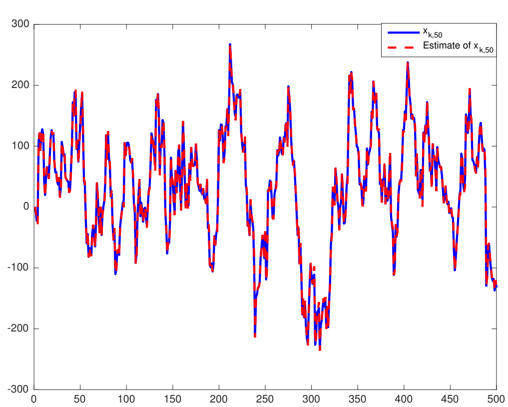

Figure 2: The state and its estimate when $a = 10$, $a_f = 0.9$, $N = 100$, $i = 50$.

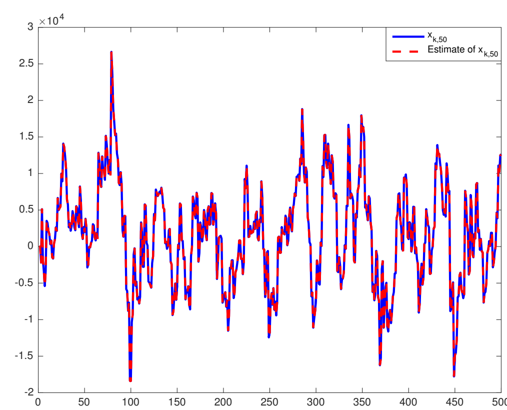

Figure 3: The state and its estimate when $a = 100$, $a_f = 0.9$, $N = 100$, $i = 50$.

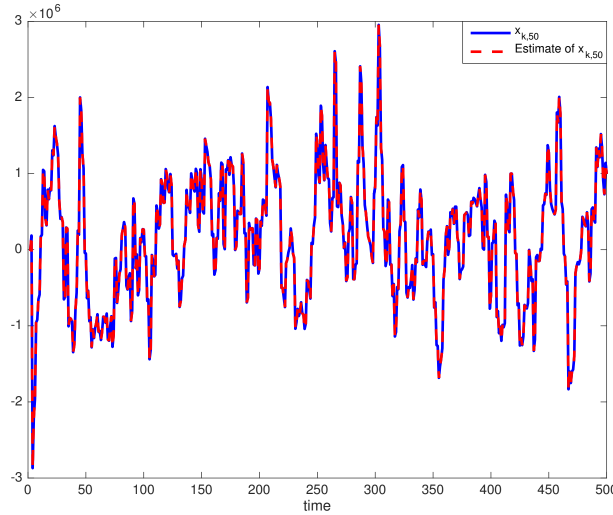

Figure 4: The state and its estimate when $a = 1000$, $a_f = 0.9$, $N = 100$, $i = 50$.

4.2 Stationarization conditions of optimum filter

It is numerically observed that the optimal bulk filter gains become asymptotically stationary for $a < \bar{a}(f, N)$ or equivalently $a < \bar{a}(a_f, N)$. We shall refer to $\bar{a}(a_f, N)$ as the stationarity threshold at a_f and N. For example, when $a = 2.5$, $f = 2$, $N = 1000$, we have:

$$K_{Bulk} = [\dots, -0.0006, 0.0015, 0.0018, 0.0615, 0.8628].$$

Note that the weights of the past measurements are getting smaller and smaller and disappear. The following index has been considered to investigate the stationarity of the Bulk Filter:

$$\Delta = \|K_{T-1}(1 : T - 1) - K_T(2 : T)\|, \tag{61}$$

where $K_k(t_1 : t_2) = (K_k(t_1), K_k(t_1 + 1), \dots K_k(t_2))$ comprises the elements from t_1 to t_2 of the bulk filter gain vector. In particular, the quantity Δ in (61) is the norm of the difference between the gains of the Bulk Filter in the last two steps of the considered time horizon $[0, T]$. If this quantity starts to increase when a is increased, it is an indication that the Bulk filter is losing its stationarity property. The values of the stationarity index Δ in (61) are reported in Figure 5 when $a_f = 0.5$ (top) and $a_f = 0.99$ (bottom) for different values of N over an horizon of $T = 1000$ steps. Moreover, the values of the thresholds $\bar{a}(a_f, N)$ and $a_m(a_f)$ for various a_f and N are reported in Table 1, where it is shown how the number of agents N affects $\bar{a}(a_f, N)$. For each fixed N, it can be observed that the threshold increases with a_f. Also, as for the dependence on N, for small values of a (namely 0.3 and 0.5) the threshold $\bar{a}(a_f, N)$ roughly decreases with N while for large values of a (namely $a = 0.8$ and $a = 0.99$) it increases. In essence, the dependence of the threshold $\bar{a}(a_f, N)$ on N remains rather weak (at least for $N \geq 100$) and the threshold is always very close to the threshold $a_m(a_f)$ where the stationary Kalman gain ceases to stabilize (1) for the considered a_f, under the naive filtering scheme (5).

Table 1: Thresholds $\bar{a}(a_f, N)$ and $a_m(a_f)$

a_f	$\bar{a}(a_f, N = 100)$	$\bar{a}(a_f, N = 1000)$	$\bar{a}(a_f, N = 10000)$	$a_m(a_f)$
0.3	2.48	2.44	2.38	2.36
0.5	2.79	2.8	2.76	2.74
0.8	3.25	3.35	3.34	3.304
0.99	3.55	3.72	3.72	3.67

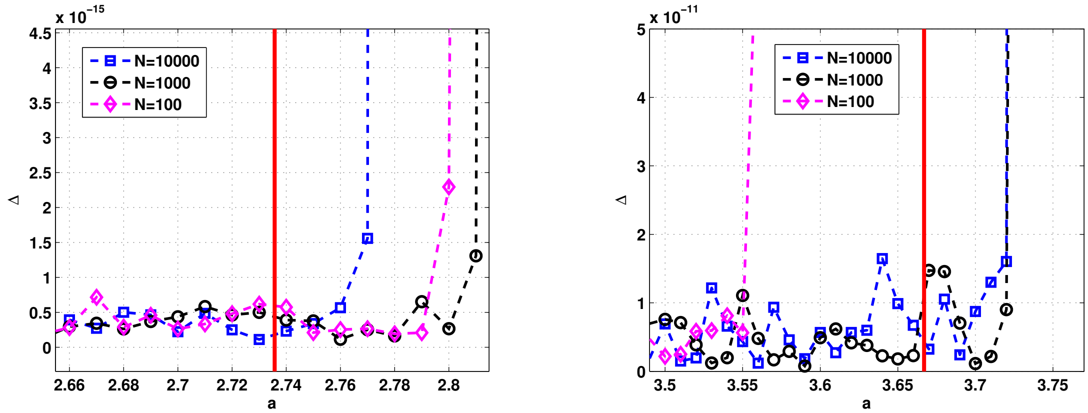

Figure 5: Stationarity index Δ as a function of a when $a_f = 0.5$ (top) and $a_f = 0.99$ (bottom), for different values of N over $T = 1000$ steps. The red vertical line represents the threshold $a_m(a_f)$ where $(K^*(a), a_f)$ ceases to belong to the stability region $S(a)$ in Figure 1.

4.3 Relation with the naive Kalman filter approach

When the Bulk filter becomes stationary, it is interesting to investigate the relation between its steady state gain coefficients and the isolated Kalman filter equivalent equations given by (54)–(57). In particular, consider the following l_2 norm based discrepancy index:

$$\delta_p = \|K_{Bulk} - K_{isolated}\|, \tag{62}$$

where $K_{isolated} = [\ldots K_3',\ K_2',\ K_1']$, with $K_j' = (a - bf)^{j-1}(1 - cK^*)^{j-1}K^*$. Figure 6 shows the discrepancy index δ_p between the Bulk Filter gains at step T and $K_{isolated}$ as a function of a when $a_f = 0.5$ (up), 0.99 (bottom), under different values of N over an horizon of $T = 1000$ steps. It is observed that the steady state bulk filter gain with mostly a few coefficients non zero could be recovered by applying the isolated Kalman filter equivalent equations given by (54)–(57) provided that N is sufficiently large. For example, when $a = 2.5,\ f = 2,\ N = 10^9$, we have:

$$K_{Bulk} = [\ldots \quad 0.0003 \quad 0.0039 \quad 0.0584 \quad 0.8650],$$

whereas the stationary Kalman filtering sequence as given by (54)–(57) is given by:

$$K_{isolated} = [\ldots \quad 0.00026616 \quad 0.0039 \quad 0.0584 \quad 0.8650].$$

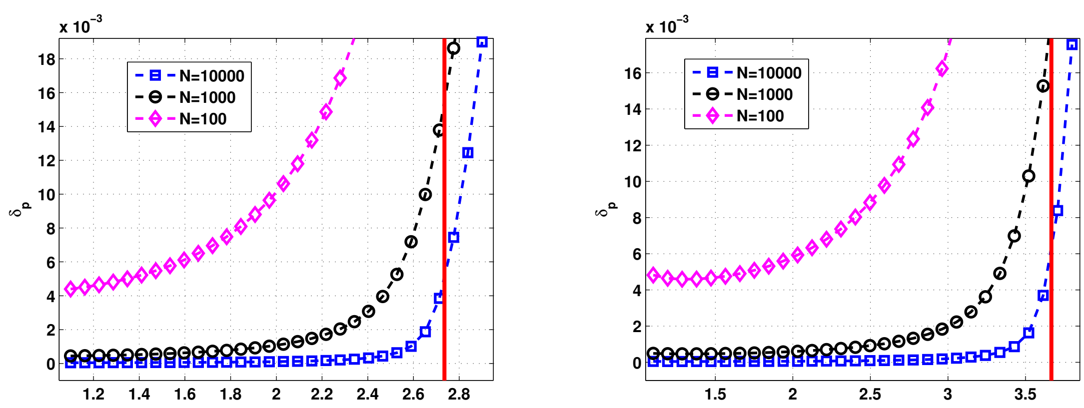

Figure 6: Discrepancy index δ_p between the Bulk Filter gains at step T and $K_{isolated}$ as a function of a when $a_f = 0.5$ (up), 0.99 (bottom), for different values of N over $T = 1000$ steps. The red vertical line represents the threshold $a_m(a_f)$ where $(K^*(a), a_f)$ ceases to belong to the stability region $S(a)$ in Figure 1.

4.4 Persistently time varying behavior for large enough a

For $a \geq \bar{a}(f, N)$ the optimal bulk filter gains remain *time-varying*. For example, when $a = 5$, $f = 4.5$, $N = 1000$. Figures 7, 8 and 9 respectively, show the last entry of K_k, the cross covariance of two arbitrary agents and the mean variance. It is observed that the gains exhibit an oscillating behavior. In fact, we know that at $a = 5$ the line $k^*(5)$ does not intersect the stability region $S(a)$ in Figure 1, and thus the naive Kalman filtering scheme cannot stabilize. When we apply the optimal Bulk filter, because of its accuracy and the stability of the closed loop dynamics, individual agent dynamics are stabilized and as long as the individual states remain weakly dependent, as N grows, the law of large numbers dictates that the interfering mean term in measurement Equation (2) go to zero. At that stage, the agents are essentially independent (notice the periodic drop in interstate correlation, Figure 8), and non interfering and the optimal filtering gain vector ultimately becomes that associated with the naive Kalman filter, i.e. stationary sequence (54)–(57), with $K^* = 0.9616$. However, we do know from Figure 1 that such a filtering scheme fails to stabilize the mean dynamics, and thus after a while, the interference term grows again, thus dominating the measurement equation and creating a growing interstate cross correlation (see Figure 8 again, and the coincidence of its peaks with those of the variance of m in Figure 9). The interdependence of states prevents the size of N from helping in knocking out interference, and the bulk filter starts again weighing more past measurements in its estimation (this can be observed in Figure 7 where the peaks of K_k roughly coincide with the minima of cross covariance terms in Figure 8). Thus persistent oscillations appear in the bulk filtering gain sequences. As the degree of instability of a increases, the period of cycles gets larger and larger as the filter has to fight longer to achieve stabilization, while the trail of non negligible coefficients associated with past measurements becomes longer. At some point, a is sufficiently large that it may become difficult to clearly distinguish cycles, and filter behavior becomes quite complex to assess, although numerically, it appears to always maintain boundedness of closed loop behavior irrespective of the size of a. Also, the dependency of closed loop behavior on N becomes non monotonic, as it contributes to worsening interference when states are correlated, and quickly diminishing it when states become weakly dependent.

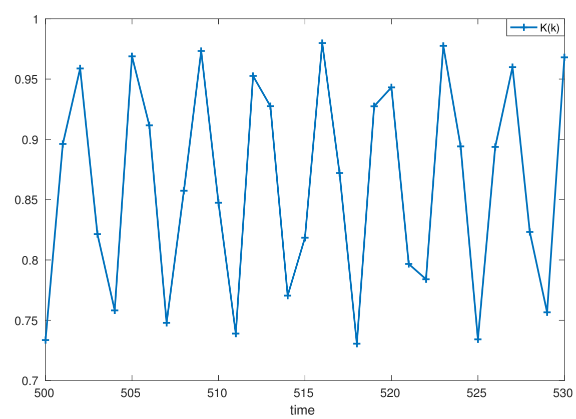

Figure 7: Last entry of K_k when $a = 5$, $f = 4.5$, $N = 1000$.

4.5 Non–optimality of the Riccati gain

It is observed that, in general, the Riccati gain f^* given by (8) is not asymptotically optimal as the number N of agents goes to infinity when using the Bulk Filter. In particular, in the range of a's for which (k^*, f) is stabilizing, the coupling term of the mean asymptotically disappears from the measurements. In that case, f^* is the optimum provided that f^* is in the range of (k^*, f) couples which still stabilize the system, and indeed the bulk filter becomes in that case equivalent to the naive Kalman filter. However, outside of the stationarization range, the quality of estimation depends on the applied feedback gain (dual effect of the control [21, 22]) and this explains the non-optimality of the Riccati gain in general. For example, Figures 10 and 11 respectively, show the average LQ cost of all the population for $a = 2$ (in stationarization region)

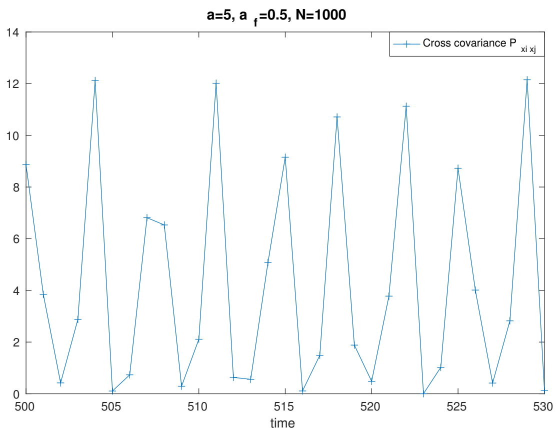

Figure 8: The cross covariance of two arbitrary agents when $a = 5$, $f = 4.5$, $N = 1000$.

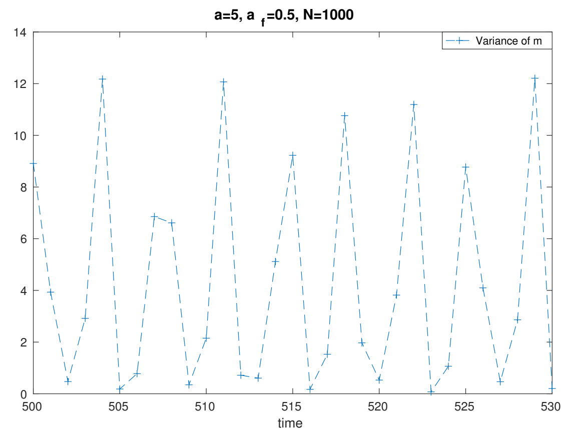

Figure 9: Mean variance when $a = 5$, $f = 4.5$, $N = 1000$.

and $a = 5$ (outside of stationarization region) using different values of N, where each point in the figures represents the average of 50 independent simulation runs and $\bigtriangledown/\bigtriangleup$ markers illustrate the standard deviation of the 50 simulations. Moreover, the vertical lines in the figures represent the Riccati gain f^*.

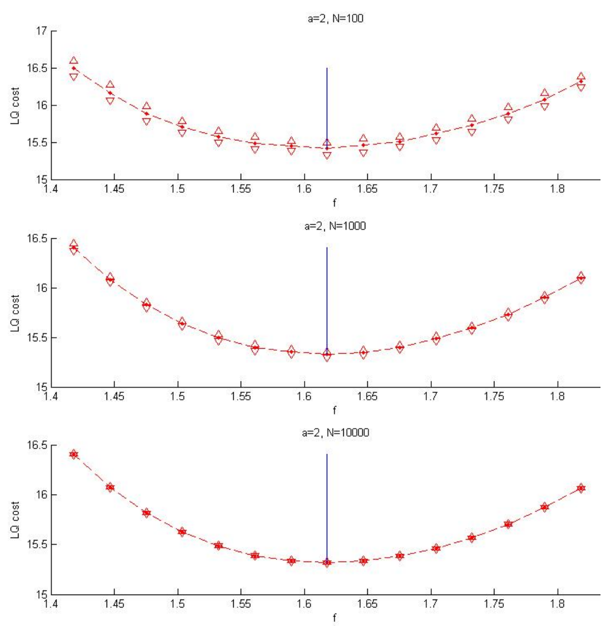

Figure 10: The average LQ cost of all the population for $a = 2$ and different values of N over $T = 1200$ steps, while the vertical blue line shows the Riccati gain f^*.

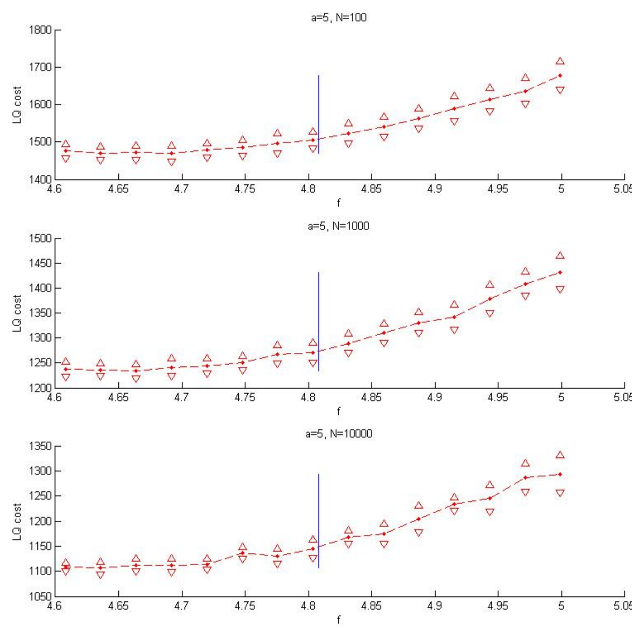

Figure 11: The average LQ cost of all the population for $a = 5$ and different values of N over $T = 1200$ steps, while the vertical blue line shows the Riccati gain f^*.

4.6 Performance of the finite memory filter approximations

Figure 12 illustrates the cost defined as $\max_i |x_{T,i}|$, $1 \leq i \leq N$, i.e. the maximum value of the agent states in the last step of the simulation (saturated at 1000), obtained by adopting the finite memory Bulk filters with memory lengths of $n = 3$, $n = 5$, $n = 10$ and $n = 50$, for different values of a and a_f. It is observed that the stabilizing capability of the approximate finite memory filter is improved by increasing the memory length n.

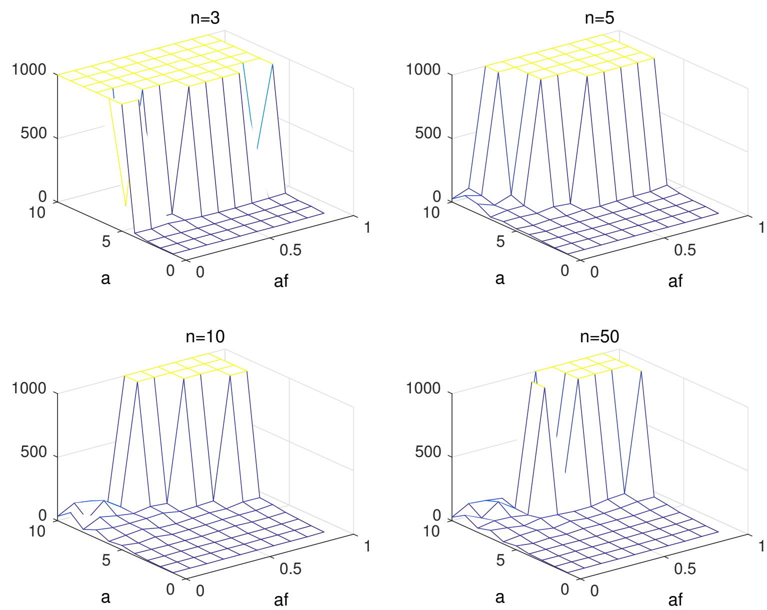

Figure 12: Simulative evaluation of the finite memory approximate Bulk filters with memory length of n when $N = 100$, $T = 1000$. The mesh reports the cost defined as $\max_i |x_{T,i}|$, $1 \le i \le N$.

5 Application to networked control systems

In [17], we presented an application example for decentralized power control in code division multiple access (CDMA) cellular telephone systems with state gain $a = 1$. In this section, we present an application example for control of multi-agent systems over a CDMA network with *arbitrary* state gain a.

Following the works in [23] and [24], we consider a model of a CDMA based communication and control system in the context of a large number of users with N users which share a channel and are assumed to be equally spaced on a circle around the base station, with a signal processing gain proportional to $1/N$. In particular, let $p_{k,i}^{(m)}$ and α denote, respectively, the transmitted power and the mean squared value of the uplink channel gain for the i^{th} mobile user of the network and let $p_{k,i}^{(b)}$ denote the received power at the base station for user i, where $p_{k,i}^{(b)} = \alpha p_{k,i}^{(m)}$. The average over slot k of the power of the CDMA signal despread by the spreading sequence of user i is given by:

$$z_{k,i} = p_{k,i}^{(b)} + \frac{h'}{N} \sum_{j \neq i}^{N} p_{k,j}^{(b)} + \sigma_{th}^2 + v_{k,i}, \tag{63}$$

where σ_{th}^2 is the variance of the background thermal noise process (modeled as a zero mean Gaussian random variable), and $v_{k,i}$ is the measurement noise due to the limited number of samples involved in the average operation (see [17, 25–27]). Note that the resulting signal processing gain is assumed to be h'/N. Also, a time slot corresponds to the time period between two consecutive power control commands. Furthermore, the actual controlling users are assumed to be independent and simply using the base station as a communication tool. They would not want to share in any way their private information in a cooperative scheme that would allow others to identify their state.

The base station itself sends the control signal to a collection of individual systems (agents). Downlink channels are considered noiseless, however the controlled individual systems are stochastic. Agents encode their (scalar) state $x_{k,i}$ by sending a power proportional to it, that is to say, $p_{k,i}^{(m)} = \beta x_{k,i}$, where β is a constant parameter. The base station in turn computes the required control based on received power which also is tainted by interference and measurement noise (as in (63)). Thus, by letting

$$y_{k,i} = z_{k,i} - \sigma_{th}^2, \quad c = \alpha\beta(1 - \frac{h'}{N}), \quad h = \alpha\beta h', \tag{64}$$

the physics of CDMA transmission viewed as a networked control system with N agents can be cast into a state space form with individual scalar dynamics described by (1) and partial observations given by (2).

6 Conclusion

In this paper, we have studied a class of certainty equivalent controllers with time invariant state estimate feedback gain for uniform agents that have linear stochastic individual dynamics and are coupled only through an interference term (the mean of all agent states), entering each of their individual measurement equations. The main challenge has been one of developing a decentralized filtering scheme under the considered class of feedback controllers. The optimum filters present several complicating features: (i) their form and performance is control dependent and thus a "dual" control effect is present; (ii) the filters are growing memory while no finite dimensional sufficient statistic appears within grasp. However, we have succeeded in developing a semi-recursive computational scheme which capitalizes on numerical results from all previous cycles, for otherwise numerical complexity rapidly explodes; (iii) It is impossible to produce a state estimate at some time k without proceeding sequentially, i.e., without having to compute filtering state estimates for all steps before k. We have numerically observed that the proposed estimator in combination with an arbitrary (stabilizing under perfect state observations) state estimate feedback gain, succeeds in maintaining the boundedness of the closed loop system even when individual systems are highly unstable. Moreover, we have established existence of a stationarity threshold $\bar{a}(f, N)$ past which, the optimal filter gains never stationarize, i.e. remain time-varying, and essentially periodic in the case of weakly unstable agents. An interpretation of such behavior was provided. Furthermore, we have derived approximate finite-dimensional filters to reduce memory requirements of the exact growing dimension filter.

In future work, we will attempt to mathematically establish the stabilization ability of our class of certainty equivalent controllers. Moreover, we will study the bulk filter properties as a dynamical system when no periodicity is apparent.

Appendix A

Proof of Theorem 1. We first note that the Bulk filter (15)–(17) is initialized with $\hat{x}_{0,i} = \bar{x}_0$, and therefore we have:

$$\mathbb{E}\left[x_{k,i}\right] = (a - bf)^k \bar{x}_0, \qquad \mathbb{E}\left[m_k\right] = (a - bf)^k \bar{x}_0, \tag{65}$$

and

$$\begin{aligned}\mathbb{E}\left[y_{k,i}\right] &= c\mathbb{E}\left[x_{k,i}\right] + h\mathbb{E}\left[m_k\right] \\ &= (c + h)(a - bf)^k \bar{x}_0.\end{aligned} \tag{66}$$

Next, we partition $P_{Y_{1,i}^k Y_{1,i}^k}$ in (17) as

$$P_{Y_{1,i}^k Y_{1,i}^k} = \begin{bmatrix} P_{Y_{1,i}^{k-1} Y_{1,i}^{k-1}} & P_{Y_{1,i}^{k-1} y_{k,i}} \\ P^T_{Y_{1,i}^{k-1} y_{k,i}} & P_{y_{k,i} y_{k,i}} \end{bmatrix}. \tag{67}$$

Then applying matrix inversion by partitioning lemma [28] we get (22). Moreover, by combining (22) and (17) we have:

$$K_k = \begin{bmatrix} P_{x_{k,i} Y_{1,i}^{k-1}} P^{-1}_{Y_{1,i}^{k-1} Y_{1,i}^{k-1}} & 0 \end{bmatrix}$$

$$+\frac{-P_{x_{k,i}Y_{1,i}^{k-1}}P^{-1}_{Y_{1,i}^{k-1}Y_{1,i}^{k-1}}P_{Y_{1,i}^{k-1}y_{k,i}}+P_{x_{k,i}y_{k,i}}}{P_{y_{k,i}y_{k,i}}-P^T_{Y_{1,i}^{k-1}y_{k,i}}P^{-1}_{Y_{1,i}^{k-1}Y_{1,i}^{k-1}}P_{Y_{1,i}^{k-1}y_{k,i}}}$$
$$\begin{bmatrix}-P^T_{Y_{1,i}^{k-1}y_{k,i}}P^{-1}_{Y_{1,i}^{k-1}Y_{1,i}^{k-1}} & 1\end{bmatrix}. \tag{68}$$

Furthermore, we note that for $t = 1, ..., k-1$

$$\begin{aligned}P_{x_{k,i}y_{t,i}} &= \mathbb{E}[(ax_{k-1,i} - bf\hat{x}_{k-1,i} + w_{k-1,i} - \mathbb{E}[x_{k,i}])\\ &(y_{t,i} - \mathbb{E}[y_{t,i}])] = aP_{x_{k-1,i}y_{t,i}} - bfK_{k-1}P_{Y_{1,i}^{k-1}y_{t,i}},\end{aligned} \tag{69}$$

therefore,

$$P_{x_{k,i}Y_{1,i}^{k-1}}P^{-1}_{Y_{1,i}^{k-1}Y_{1,i}^{k-1}} = (aP_{x_{k-1,i}Y_{1,i}^{k-1}} - bfK_{k-1} \qquad P_{Y_{1,i}^{k-1}Y_{1,i}^{k-1}})P^{-1}_{Y_{1,i}^{k-1}Y_{1,i}^{k-1}} = (a-bf)K_{k-1}. \tag{70}$$

Thus, combining (68) and (70) yields (21).

Next, we show the derivations of the covariance expressions (25)–(42). In particular, for $t = 1, \ldots, k-1$ we have:

$$\begin{aligned}P_{x_{k,i}y_{t,i}} =&\mathbb{E}[(x_{k,i} - \mathbb{E}[x_{k,i}])(y_{t,i} - \mathbb{E}[y_{t,i}])]\\ =&\mathbb{E}[(a(x_{k-1,i} - \mathbb{E}[x_{k-1,i}]) - bfK_{k-1}\\ &\begin{bmatrix} y_{1,i} - \mathbb{E}[y_{1,i}]\\ \vdots \\ y_{k-1,i} - \mathbb{E}[y_{k-1,i}]\end{bmatrix} + w_{k-1,i})(y_{t,i} - \mathbb{E}[y_{t,i}])]\end{aligned} \tag{71}$$

and for $t \geq k$ we have:

$$\begin{aligned}P_{x_{k,i}y_{t,i}} =&\mathbb{E}[(x_{k,i} - \mathbb{E}[x_{k,i}])(y_{t,i} - \mathbb{E}[y_{t,i}])]\\ =&\mathbb{E}[(x_{k,i} - \mathbb{E}[x_{k,i}])(c(x_{t,i} - \mathbb{E}[x_{t,i}])\\ &+ h(m_t - \mathbb{E}[m_t]) + v_{t,i})]\end{aligned} \tag{72}$$

thus (71) and (72) yield (25). Also,

$$\begin{aligned}P_{y_{k,i}y_{t,i}} =&\mathbb{E}[(y_{k,i} - \mathbb{E}[y_{k,i}])(y_{t,i} - \mathbb{E}[y_{t,i}])]\\ =&\mathbb{E}[(c(x_{k,i} - \mathbb{E}[x_{k,i}]) + h(m_k - \mathbb{E}[m_k])\\ &+ v_{k,i})(y_{t,i} - \mathbb{E}[y_{t,i}])]\end{aligned} \tag{73}$$

which yields (26). Moreover, for $t \leq k$ we have:

$$\begin{aligned}P_{y_{k,i}m_t} =&\mathbb{E}[(y_{k,i} - \mathbb{E}[y_{k,i}])(m_t - \mathbb{E}[m_t])]\\ =&\mathbb{E}[(c(x_{k,i} - \mathbb{E}[x_{k,i}]) + h(m_k - \mathbb{E}[m_k])\\ &+ v_{k,i})(m_t - \mathbb{E}[m_t])]\end{aligned} \tag{74}$$

and for $t > k$ we have:

$$\begin{aligned}P_{y_{k,i}m_t} =&\mathbb{E}[(y_{k,i} - \mathbb{E}[y_{k,i}])(m_t - \mathbb{E}[m_t])]\\ =&\mathbb{E}[(y_{k,i} - \mathbb{E}[y_{k,i}])(a(m_{t-1} - \mathbb{E}[m_{t-1}]) - bfK_{t-1}\\ &\begin{bmatrix}(c+h)(m_1 - \mathbb{E}[m_1]) + \tilde{v}_1\\ \vdots \\ (c+h)(m_{t-1} - \mathbb{E}[m_{t-1}]) + \tilde{v}_{t-1}\end{bmatrix} + \tilde{w}_{t-1})],\end{aligned} \tag{75}$$

thus (74) and (75) yield (27). For $t = 1, \ldots, k-1$ we have:

$$
\begin{aligned}
P_{x_{k,i}x_{t,i}} =&\mathbb{E}[(x_{k,i}-\mathbb{E}[x_{k,i}])(x_{t,i}-\mathbb{E}[x_{t,i}])] \\
=&\mathbb{E}[(a(x_{k-1,i}-\mathbb{E}[x_{k-1,i}])-bfK_{k-1} \\
&\begin{bmatrix} y_{1,i}-\mathbb{E}[y_{1,i}] \\ \vdots \\ y_{k-1,i}-\mathbb{E}[y_{k-1,i}] \end{bmatrix} + w_{k-1,i})(x_{t,i}-\mathbb{E}[x_{t,i}])]
\end{aligned} \tag{76}
$$

and for $t=k$,

$$
\begin{aligned}
P_{x_{k,i}x_{t,i}} =&\mathbb{E}[(a(x_{k-1,i}-\mathbb{E}[x_{k-1,i}])-bfK_{k-1} \\
&\begin{bmatrix} y_{1,i}-\mathbb{E}[y_{1,i}] \\ \vdots \\ y_{k-1,i}-\mathbb{E}[y_{k-1,i}] \end{bmatrix} + w_{k-1,i})^2]
\end{aligned} \tag{77}
$$

thus (76) and (77) yield (28). For $t=1,\dots,k-1$ we have:

$$
\begin{aligned}
P_{x_{k,i}m_t} =&\mathbb{E}[(x_{k,i}-\mathbb{E}[x_{k,i}])(m_t-\mathbb{E}[m_t])] \\
=&\mathbb{E}[(a(x_{k-1,i}-\mathbb{E}[x_{k-1,i}])-bfK_{k-1} \\
&\begin{bmatrix} y_{1,i}-\mathbb{E}[y_{1,i}] \\ \vdots \\ y_{k-1,i}-\mathbb{E}[y_{k-1,i}] \end{bmatrix} + w_{k-1,i})(m_t-\mathbb{E}[m_t])]
\end{aligned} \tag{78}
$$

and for $t \geq k$,

$$
\begin{aligned}
P_{x_{k,i}m_t} =&\mathbb{E}[(x_{k,i}-\mathbb{E}[x_{k,i}])(m_t-\mathbb{E}[m_t])] \\
=&\mathbb{E}[(a(x_{k-1,i}-\mathbb{E}[x_{k-1,i}])-bfK_{k-1} \\
&\begin{bmatrix} y_{1,i}-\mathbb{E}[y_{1,i}] \\ \vdots \\ y_{k-1,i}-\mathbb{E}[y_{k-1,i}] \end{bmatrix} + w_{k-1,i}) \\
&(a(m_{t-1}-\mathbb{E}[m_{t-1}])-bfK_{k-1} \\
&\begin{bmatrix} (c+h)(m_1-\mathbb{E}[m_1])+\tilde{v}_1 \\ \vdots \\ (c+h)(m_{t-1}-\mathbb{E}[m_{t-1}])+\tilde{v}_{t-1} \end{bmatrix} + \tilde{w}_{t-1})]
\end{aligned} \tag{79}
$$

thus (78) and (79) yield (29). For $t=1,\dots,k-1$ we have:

$$
\begin{aligned}
P_{m_k m_t} =&\mathbb{E}[(m_k-\mathbb{E}[m_k])(m_t-\mathbb{E}[m_t])] \\
=&\mathbb{E}[(a(m_{k-1}-\mathbb{E}[m_{k-1}])-bfK_{k-1} \\
&\begin{bmatrix} (c+h)(m_1-\mathbb{E}[m_1])+\tilde{v}_1 \\ \vdots \\ (c+h)(m_{k-1}-\mathbb{E}[m_{k-1}])+\tilde{v}_{k-1} \end{bmatrix} + \tilde{w}_{k-1})(m_t-\mathbb{E}[m_t])]
\end{aligned} \tag{80}
$$

and for $t=k$,

$$
\begin{aligned}
P_{m_k m_t} =&\mathbb{E}[(m_k-\mathbb{E}[m_k])^2] \\
=&\mathbb{E}[(a(m_{k-1}-\mathbb{E}[m_{k-1}])-bfK_{k-1} \\
&\begin{bmatrix} (c+h)(m_1-\mathbb{E}[m_1])+\tilde{v}_1 \\ \vdots \\ (c+h)(m_{k-1}-\mathbb{E}[m_{k-1}])+\tilde{v}_{k-1} \end{bmatrix} + \tilde{w}_{k-1})^2]
\end{aligned} \tag{81}
$$

thus (80) and (81) yield (30). Furthermore,

$$
\begin{aligned}
P_{y_{k,i}w_{t,i}} =& \mathbb{E}[(y_{k,i} - \mathbb{E}[y_{k,i}])w_{t,i}] \\
=& \mathbb{E}[(c(x_{k,i} - \mathbb{E}[x_{k,i}]) + h(m_k - \mathbb{E}[m_k]) \\
& + v_{k,i})w_{t,i}]
\end{aligned} \tag{82}
$$

which gives (31).

$$
\begin{aligned}
P_{m_k w_{t,i}} =& \mathbb{E}[(m_k - \mathbb{E}[m_k])w_{t,i}] \\
=& \mathbb{E}[(a(m_{k-1} - \mathbb{E}[m_{k-1}]) - bfK_{k-1} \\
& \begin{bmatrix} (c+h)(m_1 - \mathbb{E}[m_1]) + \tilde{v}_1 \\ \vdots \\ (c+h)(m_{k-1} - \mathbb{E}[m_{k-1}]) + \tilde{v}_{k-1} \end{bmatrix} + \tilde{w}_{k-1})w_{t,i}] \\
=& \mathbb{E}[aP_{m_{k-1}w_{t,i}} - bf(c+h)K_{k-1} \begin{bmatrix} P_{m_1 w_{t,i}} \\ \vdots \\ P_{m_{k-1}w_{t,i}} \end{bmatrix} + P_{\tilde{w}_{k-1}w_{t,i}}]
\end{aligned} \tag{83}
$$

which gives (32).

$$
\begin{aligned}
P_{x_{k,i}w_{t,i}} =& \mathbb{E}[(x_{k,i} - \mathbb{E}[x_{k,i}])w_{t,i}] \\
=& \mathbb{E}[(a(x_{k-1,i} - \mathbb{E}[x_{k-1,i}]) - bfK_{k-1} \\
& \begin{bmatrix} y_{1,i} - \mathbb{E}[y_{1,i}] \\ \vdots \\ y_{k-1,i} - \mathbb{E}[y_{k-1,i}] \end{bmatrix} + w_{k-1,i})w_{t,i}] \\
=& \mathbb{E}[aP_{x_{k-1,i}w_{t,i}} - bfK_{k-1} \begin{bmatrix} P_{y_{1,i}w_{t,i}} \\ \vdots \\ P_{y_{k-1,i}w_{t,i}} \end{bmatrix} + P_{w_{k-1,i}w_{t,i}}]
\end{aligned} \tag{84}
$$

which gives (33).

$$
\begin{aligned}
P_{y_{k,i}\tilde{w}_t} =& \mathbb{E}[(y_{k,i} - \mathbb{E}[y_{k,i}])\tilde{w}_t] \\
=& \mathbb{E}[(c(x_{k,i} - \mathbb{E}[x_{k,i}]) + h(m_k - \mathbb{E}[m_k]) + v_{k,i})\tilde{w}_t]
\end{aligned} \tag{85}
$$

which gives (34).

$$
\begin{aligned}
P_{m_k\tilde{w}_t} =& \mathbb{E}[(m_k - \mathbb{E}[m_k])\tilde{w}_t] \\
=& \mathbb{E}[(a(m_{k-1} - \mathbb{E}[m_{k-1}]) - bfK_{k-1} \\
& \begin{bmatrix} (c+h)(m_1 - \mathbb{E}[m_1]) + \tilde{v}_1 \\ \vdots \\ (c+h)(m_{k-1} - \mathbb{E}[m_{k-1}]) + \tilde{v}_{k-1} \end{bmatrix} + \tilde{w}_{k-1})\tilde{w}_t] \\
=& \mathbb{E}[aP_{m_{k-1}\tilde{w}_t} - bf(c+h)K_{k-1} \begin{bmatrix} P_{m_1\tilde{w}_t} \\ \vdots \\ P_{m_{k-1}\tilde{w}_t} \end{bmatrix} + P_{\tilde{w}_{k-1}\tilde{w}_t}]
\end{aligned} \tag{86}
$$

which gives (35).

$$
\begin{aligned}
P_{x_{k,i}\tilde{w}_t} =& \mathbb{E}[(x_{k,i} - \mathbb{E}[x_{k,i}])\tilde{w}_t] \\
=& \mathbb{E}[(a(x_{k-1,i} - \mathbb{E}[x_{k-1,i}]) - bfK_{k-1} \\
& \begin{bmatrix} y_{1,i} - \mathbb{E}[y_{1,i}] \\ \vdots \\ y_{k-1,i} - \mathbb{E}[y_{k-1,i}] \end{bmatrix} + w_{k-1,i})\tilde{w}_t] \\
=& \mathbb{E}[aP_{x_{k-1,i}\tilde{w}_t} - bfK_{k-1} \begin{bmatrix} P_{y_{1,i}\tilde{w}_t} \\ \vdots \\ P_{y_{k-1,i}\tilde{w}_t} \end{bmatrix} + P_{w_{k-1,i}\tilde{w}_t}]
\end{aligned} \tag{87}
$$

which gives (36).

$$
\begin{aligned}
P_{y_{k,i}v_{t,i}} =& \mathbb{E}[(y_{k,i} - \mathbb{E}[y_{k,i}])v_{t,i}] \\
=& \mathbb{E}[(c(x_{k,i} - \mathbb{E}[x_{k,i}]) + h(m_k - \mathbb{E}[m_k]) + v_{k,i})v_{t,i}]
\end{aligned} \tag{88}
$$

which gives (37).

$$
\begin{aligned}
P_{m_k v_{t,i}} =& \mathbb{E}[(m_k - \mathbb{E}[m_k])v_{t,i}] \\
=& \mathbb{E}[(a(m_{k-1} - \mathbb{E}[m_{k-1}]) - bfK_{k-1} \\
& \begin{bmatrix} (c+h)(m_1 - \mathbb{E}[m_1]) + \tilde{v}_1 \\ \vdots \\ (c+h)(m_{k-1} - \mathbb{E}[m_{k-1}]) + \tilde{v}_{k-1} \end{bmatrix} + \tilde{w}_{k-1})v_{t,i}] \\
=& aP_{m_{k-1}v_{t,i}} - bfK_{k-1} \begin{bmatrix} (c+h)P_{m_1 v_{t,i}} + P_{\tilde{v}_1 v_{t,i}} \\ \vdots \\ (c+h)P_{m_{k-1}v_{t,i}} + P_{\tilde{v}_{k-1}v_{t,i}} \end{bmatrix},
\end{aligned} \tag{89}
$$

which gives (38).

$$
\begin{aligned}
P_{x_{k,i}v_{t,i}} =& \mathbb{E}[(x_{k,i} - \mathbb{E}[x_{k,i}])v_{t,i}] \\
=& \mathbb{E}[(a(x_{k-1,i} - \mathbb{E}[x_{k-1,i}]) - bfK_{k-1} \\
& \begin{bmatrix} y_{1,i} - \mathbb{E}[y_{1,i}] \\ \vdots \\ y_{k-1,i} - \mathbb{E}[y_{k-1,i}] \end{bmatrix} + w_{k-1,i})v_{t,i}] \\
=& aP_{x_{k-1,i}v_{t,i}} - bfK_{k-1} \begin{bmatrix} P_{y_{1,i}v_{t,i}} \\ \vdots \\ P_{y_{k-1,i}v_{t,i}} \end{bmatrix}
\end{aligned} \tag{90}
$$

which gives (39).

$$
\begin{aligned}
P_{y_{k,i}\tilde{v}_t} =& \mathbb{E}[(y_{k,i} - \mathbb{E}[y_{k,i}])\tilde{v}_t] \\
=& \mathbb{E}[(c(x_{k,i} - \mathbb{E}[x_{k,i}]) + h(m_k - \mathbb{E}[m_k]) + v_{k,i})\tilde{v}_t],
\end{aligned} \tag{91}
$$

which gives (40).

$$
\begin{aligned}
P_{m_k\tilde{v}_t} =&\mathbb{E}[(m_k - \mathbb{E}[m_k])\tilde{v}_t] \\
=&\mathbb{E}[(a(m_{k-1} - \mathbb{E}[m_{k-1}]) - bfK_{k-1} \\
&\begin{bmatrix} (c+h)(m_1 - \mathbb{E}[m_1]) + \tilde{v}_1 \\ \vdots \\ (c+h)(m_{k-1} - \mathbb{E}[m_{k-1}]) + \tilde{v}_{k-1} \end{bmatrix} + \tilde{w}_{k-1})\tilde{v}_t] \\
=&aP_{m_{k-1}\tilde{v}_t} - bf(c+h)K_{k-1} \begin{bmatrix} P_{m_1\tilde{v}_t} \\ \vdots \\ P_{m_{k-1}\tilde{v}_t} \end{bmatrix} + P_{\tilde{w}_{k-1}\tilde{v}_t},
\end{aligned} \tag{92}
$$

which gives (41).

$$
\begin{aligned}
P_{x_{k,i}\tilde{v}_t} =&\mathbb{E}[(x_{k,i} - \mathbb{E}[x_{k,i}])\tilde{v}_t] \\
=&\mathbb{E}[(a(x_{k-1,i} - \mathbb{E}[x_{k-1,i}]) - bfK_{k-1} \\
&\begin{bmatrix} y_{1,i} - \mathbb{E}[y_{1,i}] \\ \vdots \\ y_{k-1,i} - \mathbb{E}[y_{k-1,i}] \end{bmatrix} + w_{k-1,i})\tilde{v}_t] \\
=&aP_{x_{k-1,i}\tilde{v}_t} - bfK_{k-1} \begin{bmatrix} P_{y_{1,i}\tilde{v}_t} \\ \vdots \\ P_{y_{k-1,i}\tilde{v}_t} \end{bmatrix} + P_{w_{k-1,i}\tilde{v}_t}
\end{aligned} \tag{93}
$$

which gives (42). This concludes the proof. □

Proof of Lemma 1. For $t = 1, \dots, k-1$ we have:

$$
\begin{aligned}
P_{x_{k,i}x_{t,j}} =&\mathbb{E}[(x_{k,i} - \mathbb{E}[x_{k,i}])(x_{t,j} - \mathbb{E}[x_{t,j}])] \\
=&\mathbb{E}[(a(x_{k-1,i} - \mathbb{E}[x_{k-1,i}]) - bfK_{k-1} \\
&\begin{bmatrix} y_{1,i} - \mathbb{E}[y_{1,i}] \\ \vdots \\ y_{k-1,i} - \mathbb{E}[y_{k-1,i}] \end{bmatrix} + w_{k-1,i})(x_{t,j} - \mathbb{E}[x_{t,j}])]
\end{aligned} \tag{94}
$$

and for $t = k$, we have:

$$
\begin{aligned}
P_{x_{k,i}x_{k,j}} =&\mathbb{E}[(a(x_{k-1,i} - \mathbb{E}[x_{k-1,i}]) - bfK_{k-1} \\
&\begin{bmatrix} y_{1,i} - \mathbb{E}[y_{1,i}] \\ \vdots \\ y_{k-1,i} - \mathbb{E}[y_{k-1,i}] \end{bmatrix} + w_{k-1,i})(a(x_{k-1,j} - \mathbb{E}[x_{k-1,j}]) - bfK_{k-1} \\
&\begin{bmatrix} y_{1,j} - \mathbb{E}[y_{1,j}] \\ \vdots \\ y_{k-1,j} - \mathbb{E}[y_{k-1,j}] \end{bmatrix} + w_{k-1,j})]
\end{aligned} \tag{95}
$$

thus (94) and (95) yield (43). The rest of the proof is similar to that of Theorem 1. □

Proof of Theorem 2. First, we partition $P_{Y^k_{k-l,i}Y^k_{k-l,i}}$ in (49) as follows:

$$
P_{Y^k_{k-l,i}Y^k_{k-l,i}} = \begin{bmatrix} P_{y_{k-l,i}y_{k-l,i}} & P_{y_{k-l,i}Y^k_{k-l+1,i}} \\ P^T_{y_{k-l,i}Y^k_{k-l+1,i}} & P_{Y^k_{k-l+1,i}Y^k_{k-l+1,i}} \end{bmatrix}. \tag{96}
$$

Then applying matrix inversion by partitioning lemma [28] we get (52). Moreover, combining (49) and (52) yields (51). The rest of the proof is similar to that of Theorem 1. □

References

[1] C. Y. Chong and S. P. Kumar, "Sensor networks: evolution, opportunities, and challenges," Proceedings of the IEEE, 91(8)1247–1256, 2003.

[2] J. H. Reif and H. Y. Wang, "Social potential fields: A distributed behavioral control for autonomous robots," Robotics and Autonomous Systems, 27(3)171–194, 1999.

[3] E. L. Karfopoulos and N. D. Hatziargyriou, "A multi-agent system for controlled charging of a large population of electric vehicles," IEEE Transactions on Power Systems, 28(2)1196–1204, 2013.

[4] H. Yin, P. G. Mehta, S. P. Meyn, and U. V. Shanbhag, "Synchronization of coupled oscillators is a game," IEEE Transactions on Automatic Control, 57(4)920–935, 2012.

[5] D. Grönbaum and A. Okubo, "Modelling social animal aggregations," in Frontiers in theoretical biology. New York: Springer-Verlag, 1994, 296–325.

[6] K. M. Passino, "Biomimicry of bacterial foraging for distributed optimization and control," IEEE Control Systems Magazine, 22(3)52–67, 2002.

[7] D. Helbing, I. Farkas, and T. Vicsek, "Simulating dynamical features of escape panic," Nature, 407(6803)487–490, 2000.

[8] A. Lachapelle, "Human crowds and groups interactions: a mean field games approach," Technical report, CEREMADE, Université Paris-Dauphine, 2010.

[9] E. Altman, T. Boulogne, R. El-Azouzi, T. Jiménez, and L. Wynter, "A survey on networking games in telecommunications," Computers and Operations Research, 33(2)286–311, 2006.

[10] S. Roshany-Yamchi, M. Cychowski, R. R. Negenborn, B. D. Schutter, K. Delaney, and J. Connell, "Kalman filter-based distributed predictive control of large-scale multi-rate systems: application to power networks," IEEE Transactions on Control Systems Technology, 21(1)27–39, 2013.

[11] R. Vadigepalli and F. J. Doyle, "A distributed state estimation and control algorithm for plantwide processes," IEEE Transactions on Control Systems Technology, 11(1)119–127, 2003.

[12] P. E. Caines and A. C. Kizilkale, "ϵ-nash equilibria for partially observed lqg mean field games with a major player," IEEE Transactions on Automatic Control, 2016.

[13] ——, "Recursive estimation of common partially observed disturbances in mfg systems with application to large scale power markets," in Proc. of the 52nd IEEE conference on decision and control, 2013, 2505–2512.

[14] ——, "Mean field estimation for partially observed lqg systems with major and minor agents," In Proc. of the 19th IFAC world congress, 2014.

[15] M. Huang, P. E. Caines, and R. P. Malhamé, "Distributed multi-agent decision-making with partial observations: asymptotic nash equilibria," in Proc. of the 17th international symposium on mathematical theory of networks and systems, Kyoto, Japan, 2006, 2725–2730.

[16] B. C. Wang and J. F. Zhang, "Distributed output feedback control of markov jump multi-agent systems," Automatica, 49(5)1397–1402, 2013.

[17] M. Abedinpour-Fallah, R. Malhamé, and F. Martinelli, "A class of interference induced games: Asymptotic nash equilibria and parameterized cooperative solutions," Automatica, 69, 181–194, 2016.

[18] A. Bagchi, Optimal control of stochastic systems. Prentice-Hall, Inc., 1993.

[19] M. Abedinpour-Fallah, R. P. Malhamé, and F. Martinelli, "Decentralized estimation in a class of measurements induced mean field control problems," in Proc. of the 52nd IEEE conference on decision and control, 2013, 3146–3151.

[20] D. G. Manolakis, V. K. Ingle, and S. M. Kogon, Statistical and adaptive signal processing: spectral estimation, signal modeling, adaptive filtering, and array processing. Artech House Norwood, 2005, 46.

[21] A. A. Feldbaum, "Dual control theory i-iv," Autom. Remote Control, 21(6)874–880, 1960.

[22] H. S. Witsenhausen, "A counterexample in stochastic optimum control," SIAM Journal on Control, 6(1)131–147, 1968.

[23] D. Tse and S. Hanly, "Linear multiuser receivers: Effective interference, effective bandwidth and user capacity," IEEE Transactions on Information Theory, 45(2)641–657, 1999.

[24] S. Verdú and S. Shamai, "Spectral efficiency of cdma with random spreading," IEEE Transactions on Information Theory, 45(2)622–640, 1999.

[25] S. Perreau and M. D. Anderson, "A new method for centralised and decentralised robust power control in cdma systems," Digital Signal Processing, 16(5)568–576, 2006.

[26] S. Koskie and Z. Gajic, "Signal-to-interference-based power control for wireless networks: A survey, 1992–2005," Dynamics of Continuous, Discrete and Impulsive Systems B: Applications and Algorithms, 13(2)187–220, 2006.

[27] M. Huang, P. E. Caines, and R. P. Malhamé, "Uplink power adjustment in wireless communication systems: a stochastic control analysis," IEEE Transactions on Automatic Control, 49(10)1693–1708, 2004.

[28] B. Noble and J. W. Daniel, Applied linear algebra. Prentice Hall, Englewood Cliffs, NJ, 1988.